Description and Comprehensive Analysis of the Mancos Shale, Uinta Basin, U. S. A.

Xueke Chang

400006246

Research Supervisor: Dr. Janok Bhattacharya

A proposal submitted to the School of Geography and Earth Sciences, McMaster University, in partial fulfillment of the requirements for the degree of

Bachelor of Science

Introduction

Over the past decades, heterogeneous sedimentary rocks and their related sedimentary structures, ichnofacies (Droser and Bottjer, 1993; Savrda et al., 1984; Savrda and Bottjer, 1991; Taylor and Goldring, 1993), comprehensive depositional processes and settling environments (Fan, 2013; Lazar et al., 2015; Wilson and Schieber, 2014) have been investigated by geologists, for reconstructing past environments and climate (Algeo et al., 2004) and making correlations between different outcrops (Campbell, 1967). Fine grained sediments, with grain size smaller than 63 μm, are the most abundant sediments on Earth's surface (Li and Schieber, 2018; Macquaker et al., 2010). Mud also has an economic advantage because it stores ore deposits and acts as oil and gas reservoirs (Broadhead, 2015; Gentzis, 2013).

Even though many surveys have been conducted on mud-dominated sediments and rocks, their transportation and depositional mechanisms are still under debate. Previous models suggest that most muds are deposited under suspension in low energy and quiet environments, (Birgenheier et al., 2017; Li and Schieber, 2018; Macquaker and Bohacs, 2007) while recent studies point out that processes such as hyperpycnal flows (Bhattacharya and MacEachern, 2009; Birgenheier et al., 2017; Mulder et al, 2003; Wilson and Schieber, 2014), wave-enhanced sediment-gravity-flows (Macquaker et al., 2010), tempestites (Myrow and Southard, 1996), and turbidites (Li and Schieber, 2018) are capable of offshore flocculated muddy sediment transportation and deposition along continental shelves (Schieber, 2016).

This research will provide a detailed facies analysis of the Upper Mancos Shale from the Uinta Basin, Utah, which was formed during the late Cretaceous period. The mud-dominated Mancos Shale Formation, which is composed of interbedded sand, silt and clay, is of research interest because it was deposited in a muddy shelf environment in an epicontinental sea (Li and Schieber, 2018). It preserved various sedimentary structures (ripples, laminations, etc.) that allow interpretation of sediment transportation mechanisms (Birgenheier et al., 2017; Hart, 2016). It also recorded transgression-regression cycles during the Cretaceous (Birgenheier et al., 2017; Hart, 2016).

The Cretaceous is documented to be a warm period due to greenhouse effects (Dennis et al., 2013; Otto-Bliesner et al., 2002), followed by a global cooling during the Late Campanian and Maastrichtian (75 to 65 million years ago). Theoretically, warmer climates generate more intense storm events because high temperature is highly correlated to high atmospheric energy. By studying Cretaceous sediments, such as the Mancos Shale Formation, it is expected to analyse storm events relative to the sedimentation rate from the observed sedimentary structures. Investigations on Cretaceous sediments contribute to the reconstruction of past environments and climate models, and therefore scientists are able to compare and contrast them with modern climates. In addition, the Mancos Shale is considered to be thermally mature and full of reservoirs of organic matter, which has been producing gas and oil since the last century (Broadhead, 2015; Gentzis, 2013).

Geologic Setting

This sample was extracted from Upper Mancos Shale in the Uinta Basin, Utah. Since the exact location and which member it belongs to is unknown, a general description of the Mancos Shale in Uinta Basin is provided (Grigg, 2016).

The Mancos Shale was formed during the Late Cretaceous Period, originally deposited on a foreland basin in the Western Interior Seaway (Broadhead, 2015; Hawkins et al., 2016; Mack et al., 2016; Pasley and Riley, 1993; Ridgley et al., 2013). Thickness of the Mancos Shale is over 5000 feet in the Uinta Basin (Grigg, 2016; Hettinger and Kirschbaum, 2003). During the Cretaceous, the geological structure of western North America was mainly affected by the Sevier-Laramide orogenies (Livaccari, 1991; McCauley, 2013). The Sevier Orogeny generated sediments that formed the Mancos Shale (Grigg, 2016; Hettinger and Kirschbaum, 2003). It was marked by thrust faults oriented north-south which lead to the creation of the foreland basin and the basin became the Interior Seaway when sea-level increased (Livaccari, 1991; McCauley, 2013). Thrust faults continued, and migrated toward the east, resulting in an unconformity between the Mancos Shale and underlying Dakota Sandstone (McCauley, 2013; Ridgley et al., 2013). The Mancos Shale was then structurally deformed by a compression during the Laramide Orogeny (late Cretaceous to early Tertiary) and divided into several Laramide Rocky Mountain subbasins, including the Uinta Basin (Broadhead, 2015; Hawkins et al., 2016).

In the Uinta Basin, the Mancos Shale is subdivided into 5 members (see Fig 1. by McCauley, 2013) which represent the age from mid-Turonian to Campanian. The basal Tununk Shale overlies the mid-Turonian unconformity, followed by deposition of the Juana Lopez Member, the Blue Gate Shale, the Prairie Canyon and the youngest Buck Tongue, which record proximal marine to continental and distal marine sandstones and shales (McCauley, 2013).

Background Literature

Schieber (2016) modified a graph (see Fig 2.) which illustrates how the slopes of the shelf are related to corresponding sediment transportation processes. These bottom processes (wave/tide/storm currents, hyperpycnal flows, sediment-gravity-flows, etc.) are energetic (Hart, 2016) and generate distinctive facies. Hart (2016) provided a diagram illustrating how sediments vary from proximal (shoreline) to distal (basin) with different mechanisms, marine organic matter (MOM) and climate (see Fig 3.). Li and Schieber (2018) also demonstrated a depositional model of the Tununk Shale Member in the Mancos Shale (see Fig 4.) In general, sediments become finer basinward with less siliciclastic and more organic content.

Hyperpycnal flows appear when river water has a higher density than sea water it is entering (Mulder et al., 2003) and is usually generated when there is increased sediment concentration in the flow (see Fig 5.). In sedimentary records this type of flow is indicated with reverse and normal grading which represents waxing and waning flows (Bhattacharya and MacEachern, 2009). Hyperpycnal flows are able to transport sediment over slope of 0.7° or larger up to 100 km (Birgenheier et al., 2017; Schieber, 2016) and therefore are not likely the main mechanism for long-distance offshore sediment transportation. Birgenheier et al. (2017) refer to this type of flow as river-fed bottom currents while discussing offshore depositional models of the Blue Gate Member in the Mancos Shale.

Wave-enhanced sediment-gravity-flow is another process explained by Macquaker et al. (2010) which is able to move sediment offshore in low slopes (Birgenheier et al., 2017). Macquaker et al. (2010) summarized a facies model for this type of flow (WESGF) which has three main components (see Fig 6.). The erosional basal lamina set unit A may contain curved ripple laminations, overlain by unit B, which is composed of silt and clay with wave laminations (Macquaker et al., 2010) and is an indicator of mixing between coarser sediments in unit A with finer sediments transported by WESGF. Unit C comprises the sediments deposited as a fluid mud. In outcrops this is shown as fining upward units (Macquaker et al., 2010).

According to Mulder and Alexander (2001), turbidity currents are surge-like sedimentary density flows, with less than 10% concentration of sediments. These currents occur on higher slopes (see Fig 2.) and can produce Bouma Sequence (see Fig 7.). According to Shanmugam (1997), Bouma Sequence describes a fining upward sequence with an erosional surface, massive sandy Ta layer, graded, laminated sand to silt middle layers (Tb, Tc, Td) as well as Te, which deposited as suspended mud.

Tempestites are deposits of storm-generated flows (Myrow and Southard, 1996). In sedimentary records, tempestites show a sequence of an erosional surface overlain by hummocky-cross-stratified sand, and combined-flow rippled fine sand with laminated mud on top (see Fig 8.). This model is summarized by Suter (2006). Wave ripples are also indicators of storm events.

Tidal or wind currents are likely important for transporting sediments along interior epicontinental seaways (Schieber, 2016) as they occur on relatively shallow slopes (see Fig 2.). Fan (2013) proposed that in sediment records, rhythmic-laminated mud and sand alteration are typical sign of tidal influence. An example of tidal lamina is shown in Fig. 9, suggesting tides may be partly responsible for sediment transport in the Mancos Shale (Genovese, 2017).

Objectives

This research aims to provide a detailed sedimentological analysis of the Cretaceous Mancos Shale sample and to have a better understanding of its depositional environment by 1) identifying any transportation and depositional processes based on sedimentary structures observed on this sample; 2) estimating sediment accumulation rate and oxygen level of the Mancos Shale depositional environment. Existing mud-dominated shelf facies models and ichnofacies models will be used to compare with the results to draw conclusions.

Working Hypothesis

The Mancos Shale sample will be analyzed to see if it was deposited on a continental shelf (distal marine), whether the sedimentary structures match existing facies models of wave-enhanced sediment-gravity flows, turbidites, storms and tides and if this sample recorded rhythmic tidal influence. Bioturbation and trace fossils will be studied to determine the sedimentation rate and oxygen level of the settling environment.

Methods & Analysis

A 30 cm-long sample taken from the Mancos Shale outcrop in the Uinta Basin, Utah is analyzed in centimeter to millimeter scale. It is covered by wax in order to preserve its geomechanical properties (Grigg, 2016). A binocular scope and scanner are used to retrieve high-resolution pictures of the sample core. A microscope will be used to observe millimeter-scale sedimentary structures. Pictures will be labelled using graphic software such as Adobe Illustrator. Grain sizes, sedimentary structures such as laminations, ripples, grading and ichnofacies will be identified and documented by constructing a high-resolution measured section via Adobe Illustrator. Degree of bioturbation will be examined using the bioturbation index table (see Fig 10.) by Taylor and Goldring (1993). Ichnofacies observed will be compared to previous models from Savrda and Bottjer (1991) for analysis and interpretation of oxygen level at the time of deposition.

Possible transportation and depositional processes, such as wave-enhanced sediment-gravity flows, will be interpreted by comparing results with existing mud-dominated shelf facies models for better understanding of mud-deposition on distal continental shelves. Thickness of each lamina will be recorded to see if any periodic pattern is shown. Proportion of different transportation mechanisms will be estimated to determine which processes are responsible for dominant sediment transportation in this Mancos Shale.

Figure 11 is a picture of the entire sample. Figure 12 and Figure 13 show wave ripples and laminations respectively. This sample reveals different possible offshore transportation mechanisms (storm or tide currents) and different trace fossils. Degree of bioturbation is not constant throughout the sample.

Timeline

The first component of this research is the meeting between the supervisor and the student which was done in September 14, 2018. After that, the first draft of research proposal will be handed in before October 5th, 2018. The second component is the literature review which is due November 2nd, 2018. The active research occupies the months until February 22, 2019 while the full draft of the final thesis is due March 15, 2019. After the first draft, the final written thesis will be handed in no later than April 9, 2019 following by the final component, paper presentation on April 10, 2019.

Appendix

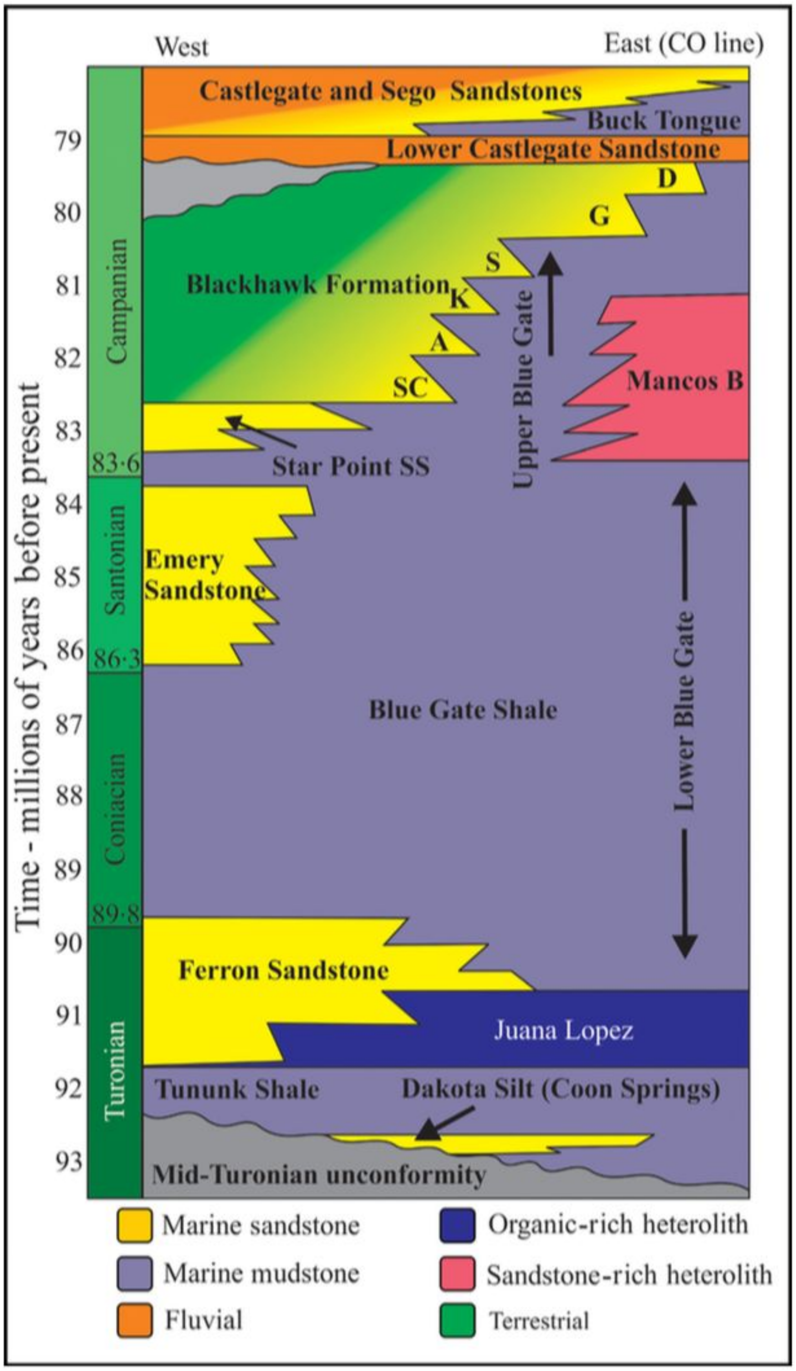

Figure 1. Stratigraphy of Mancos Shale and other formations from Uinta Basin, Utah. Blackhawk Formation members are: SC=Spring Canyon; A=Aberdeen; K=Kenilworth; S=Sunnyside; G=Grassy; D=Desert. Taken from Birgenheier et al. (2013).

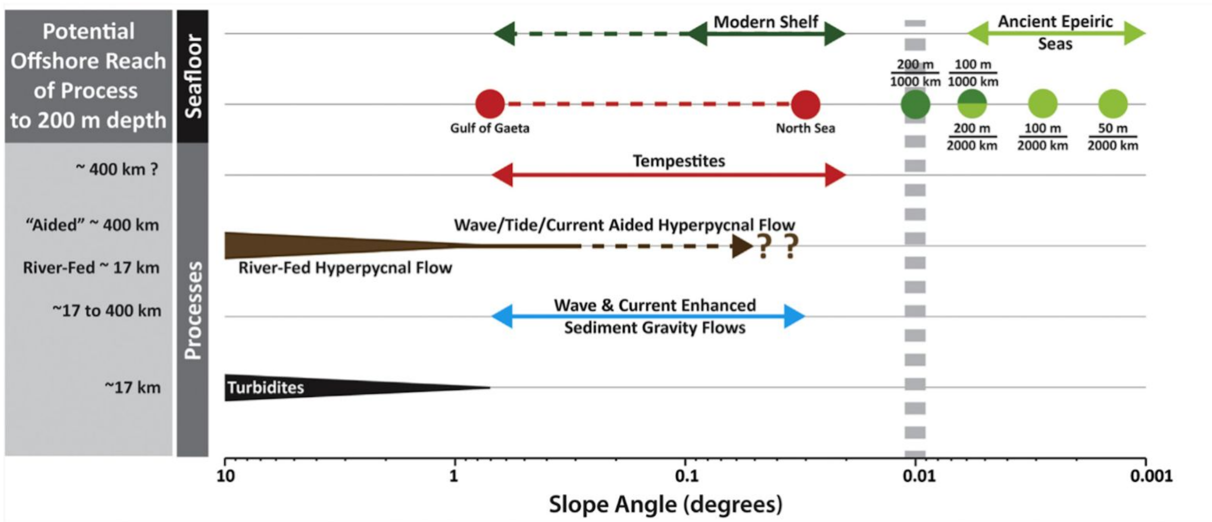

Figure 2. Relationship between sediment transportation processes and slope of seafloor by Schieber (2016).

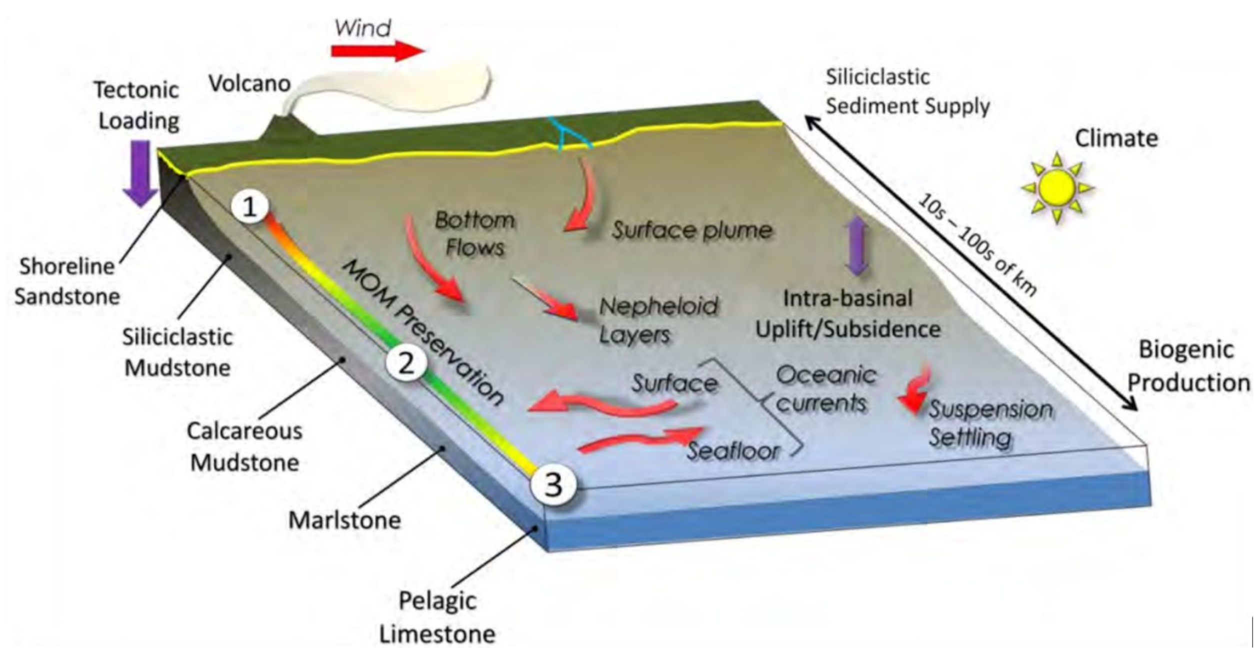

Figure 3. A conceptual model taken from Hart (2016) showing how lithologies and organic content change from shoreline to distal shelf in an epicontinental sea, and where different mechanisms appear.

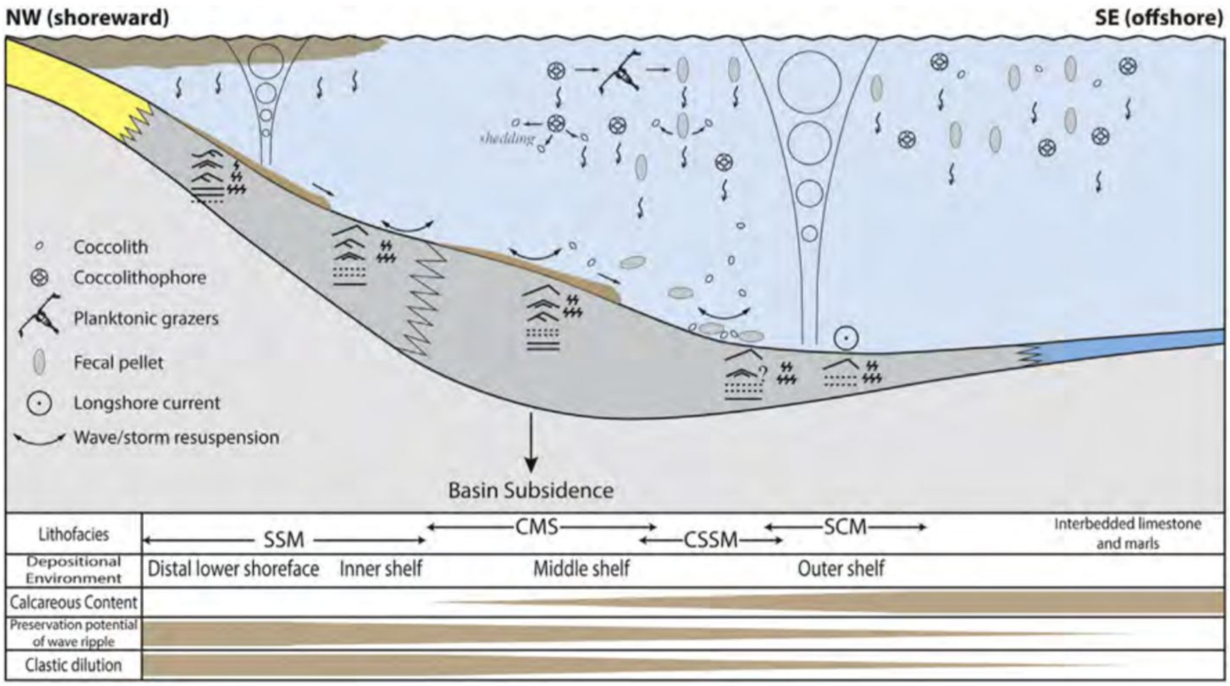

Figure 4. Cross-sectional graph of depositional model of Tununk Shale (CSSM = Carbonate-bearing, silty and sandy mudstone, SSM = Non-calcareous, silty and sandy mudstone, CMS = Carbonate-bearing, silty mudstone to muddy siltstone, SCM = Silty-bearing, calcareous mudstone). Please refer to Fig 4.1 for labels. Taken from Li and Schieber (2018).

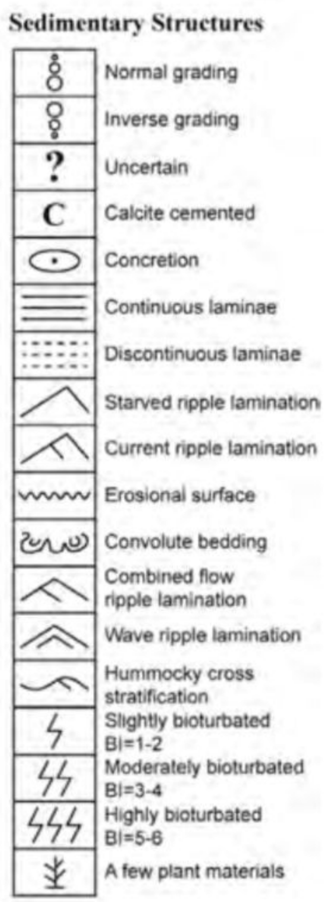

Figure 4.1. Labels to Figure 4. Taken from Li and Schieber (2018).

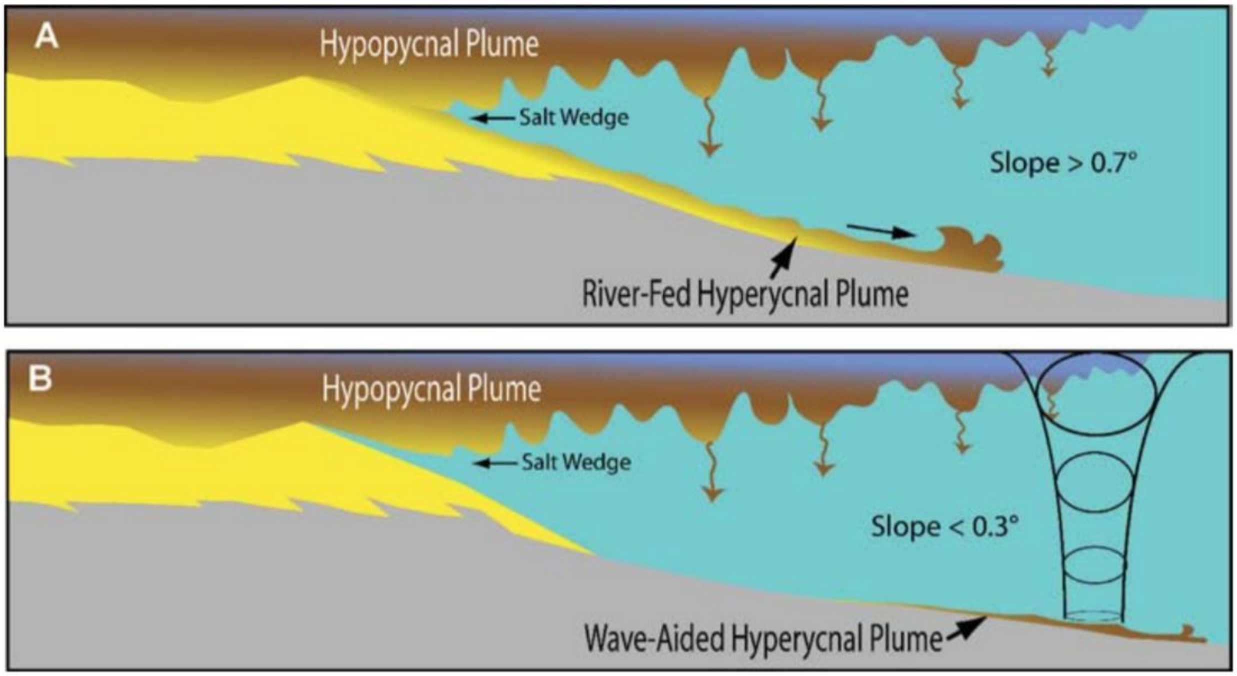

Figure 5. Hyperpycnal and hypopycnal plumes by Bhattacharya and MacEachern (2009).

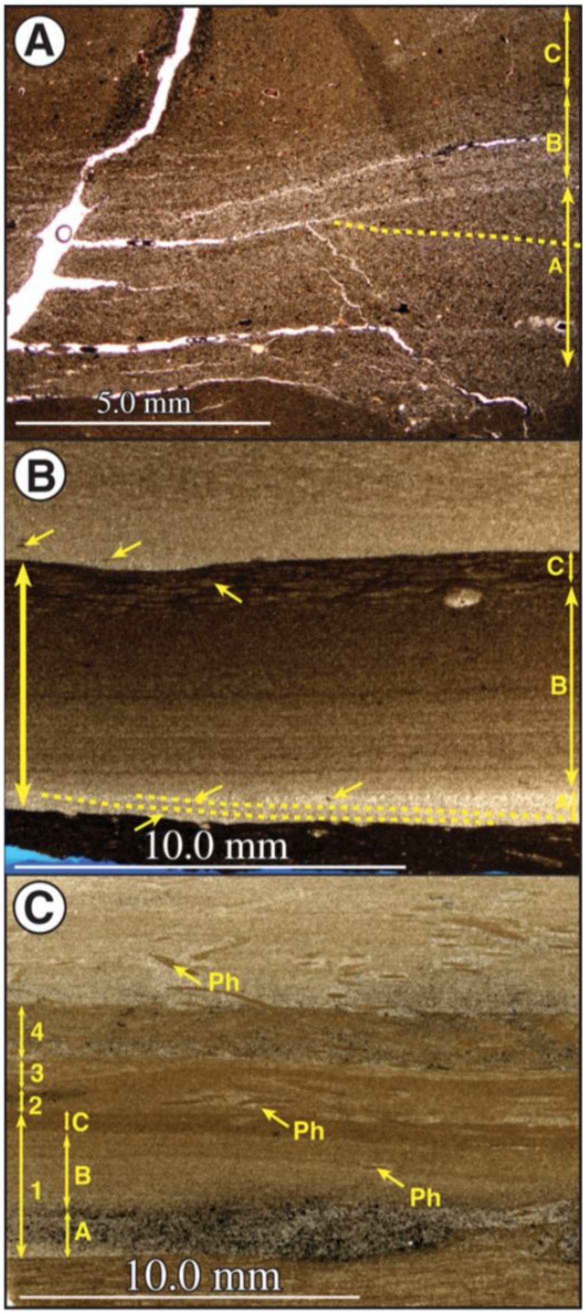

Figure 6. Graphs showing three-part WESGF in sediments by Macquaker et al. (2010). A is from Eel Shelf, B is from Mowry Shale, Wyoming and C is from Cleveland Ironstone, UK. A, B and C in graphs represent basal lamina unit, laminated interbed, burrowed clay drapes respectively. Phycosiphon [Ph] are shown. Overall it is normally graded.

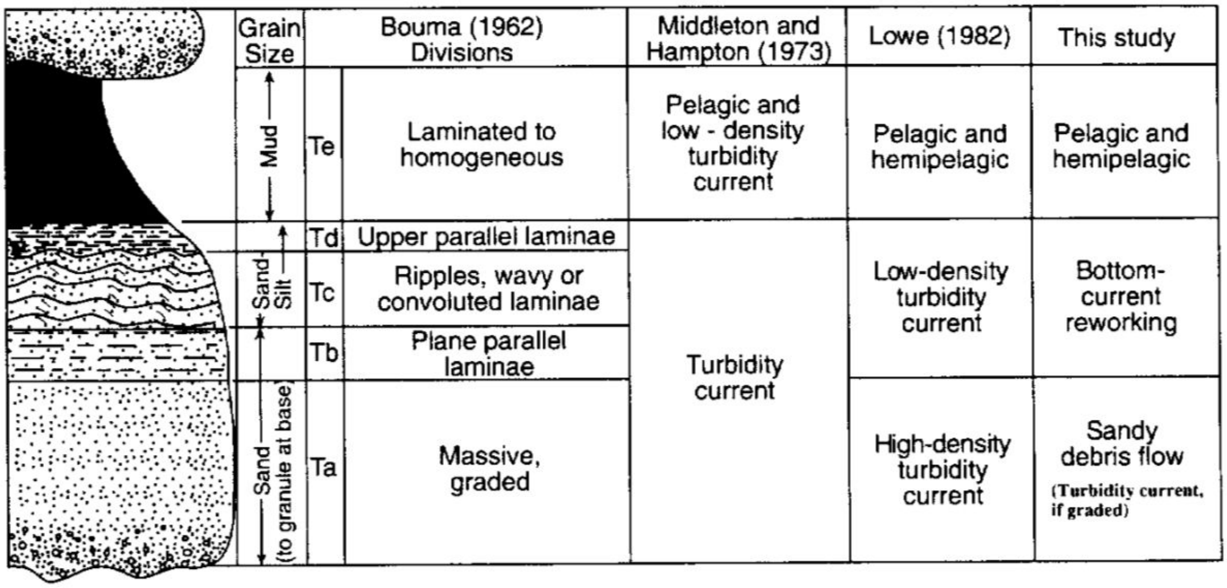

Figure 7. Modified Bouma Sequence diagram by Shanmugam (1997).

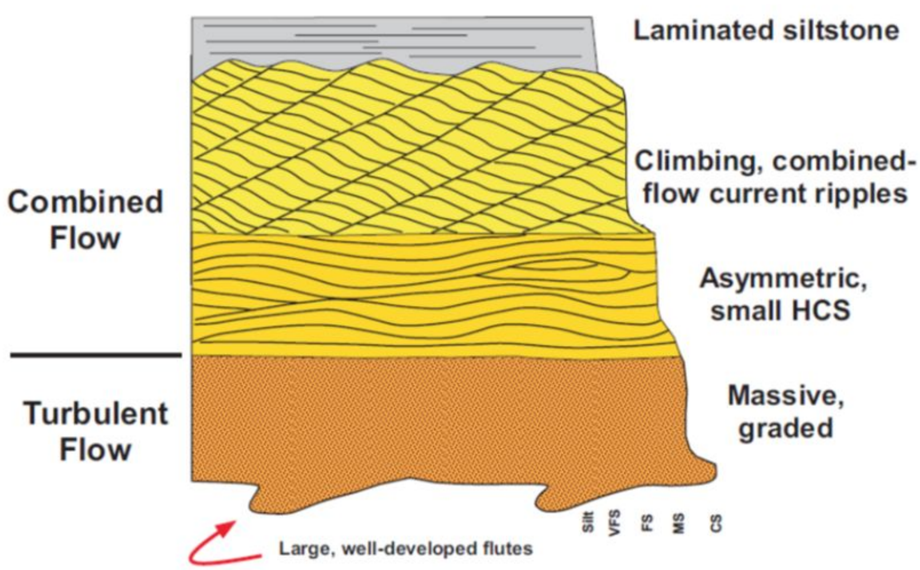

Figure 8. A model of typical tempestite deposition, taken from Suter (2006).

Figure 9. Rhythmic laminations of sand and clay in Upper Mancos Shale, New Mexico. Taken from Genovese (2017).

Grade	Percent bioturbated	Classification
0	0	No bioturbation
1	1–4	Sparse bioturbation, bedding distinct, few discrete traces and/or escape structures
2	5–30	Low bioturbation, bedding distinct, low trace density, escape structures often common
3	31–60	Moderate bioturbation, bedding boundaries sharp, traces discrete, overlap rare
4	61–90	High bioturbation, bedding boundaries indistinct, high trace density with overlap common
5	91–99	Intense bioturbation, bedding completely disturbed (just visible), limited reworking, later burrows discrete
6	100	Complete bioturbation, sediment reworking due to repeated overprinting

Figure 10. Description of bioturbation index by Taylor and Goldring (1993).

Figure 11. The Mancos Shale Sample.

Figure 12. Wave ripples.

Figure 13. Laminated fine sand and mud alteration, might be rhythmic and show tidal influence.

White bar is equivalent to 1 centimeter. On the top of this picture, laminates are bioturbated.

References

Algeo T. J., Schwark L. and Hower J. C. (2004) High-resolution geochemistry and sequence stratigraphy of the Hushpuckney Shale (Swope Formation, eastern Kansas): implication for climato-environmental dynamics of the Late Pennsylvanian Midcontinent Seaway. *Chemical Geology* 206(3-4), 259-288.

Bhattacharya J. P. and MacEachern J. A. (2009) Hyperpycnal Rivers and Prodeltaic Shelves in the Cretaceous Seaway of North America. *J. Sediment. Res.* 79(4), 184-209.

Birgenheier L. P., Horton B., McCauley A. D., Johnson C. L. and Kennedy A. (2017) A depositional model for offshore deposits of the lower Blue Gate Member, Mancos Shale, Uinta Basin, Utah, USA. *Sedimentology* 64, 1402-1438.

Broadhead R. F. (2015) The Upper Mancos Shale in the San Juan Basin: Three plays, Conventional and Unconventional. *Search and Discovery Article* 10791.

Campbell C. V. (1967) Lamina, Laminaset, Bed and Bedset. *Sedimentology* 8(1), 7-26.

Dennis K. J., Cochran J. K., Landman N. H. and Schrag D. P. (2013) The climate of the Late Cretaceous: New insights from the application of the carbonate clumped isotope thermometer to Western Interior Seaway macrofossil. *Earth Planet. Sci. Lett.* 362, 51-65.

Droser M. L. and Bottjer D. J. (1993) Trends and Patterns of Phanerozoic Ichnofabrics. *Annu. Rev. Earth Planet. Sci.* 21, 205-225.

Fan D. (2013) Classifications, sedimentary features and facies associations of tidal flats. *Journal of Paleogeography* 2(1), 66-80.

Genovese C. (2017) Detailed Thin-bedded Facies Analysis of Mancos C in the Upper Mancos Shale, New Mexico. McMaster University MS. Thesis

Gentzis T. (2013) A review of the thermal maturity and hydrocarbon potential of the Mancos and Lewis shales in parts of New Mexico, USA. *International Journal of Coal Geology* 113, 64-75.

Grigg J. J. (2016) Macroscopic and Microscopic Controls on Mechanical Properties of Mudstones. New Mexico Institute of Mining and Technology MS. Thesis.

Hart B. S. (2016) Marine mudstone source rocks in epicontinental basins: Development of a conceptual facies model and application to Cenomanian/Turonian mudstones of the Cretaceous Western Interior Seaway in Dolan M. P., Higley D. K. and Lillis P. G., Hydrocarbon Source Rocks in Unconventional Plays, Rocky Mountain Region. The Rocky Mountain Association of Geologists.

Hawkins S. J., Charpentier R. R., Schenk C. J., Leathers-Miller H. M., Klett T. R., Brownfield M. E., Finn T. M., Gaswirth S. B., Marra K. R., Le P. A., Mercier T. J., Pitman J. K. and Tennyson M. E. (2016) Assessment of continuous (unconventional) oil and gas resources in the Late Cretaceous Mancos Shale of the Piceance Basin, Uinta-Piceance Province, Colorado and Utah, 2016: U.S. Geological Survey Fact Sheet 2016-3030, 4 p., http://dx.doi.org/10.3133/fs201 63030.

Hettinger R. D. and Kirschbaum M. A. (2003) Stratigraphy of the Upper Cretaceous Mancos Shale (upper part) and Mesaverde Group in the southern part of the Uinta and Piceance basins, Utah and Colorado in Petroleum Systems and Geologic Assessment of Oil and Gas in the Uinta-Piceance Province, Utah and Colorado, U. S. Geological Survey Digital Data Series DDS-69-B.

Lazar R. O., Bohacs K. M., Macquaker J. H. S., Schieber J. and Demko T. M. (2015) Capturing Key Attributes of Fine-Grained Sedimentary Rocks in Outcrops, Cores, and Thin Sections: Nomenclature and Description Guidelines. *J. Sediment. Res.* 85, 230-246.

Li Z. and Schieber J. (2018) Detailed facies analysis of the Upper Cretaceous Tununk Shale Member, Henry Mountains Region, Utah: Implications for mudstone depositional models in epicontinental seas. *Sediment. Geol.* 364, 141-159.

Livaccari R. F. (1991) Role of crustal thickening and extensional collapse in the tectonic evolution of the Sevier-Laramide orogeny, western United States. *Geology* 19(11), 1104-1107.

Mack G. H., Hook S., Giles K. A. and Cobban W. A. (2016) Sequence stratigraphy of the Mancos Shale, lower Tres Hermanos Formation, and coeval middle Cenomanian to middle Turonian strata, southern New Mexico, USA. *Sedimentology* 63(4), 781-808.

Macquaker J. H. S., Bentley S. J. and Bohacs K. M. (2010) Wave-enhanced sediment-gravity flows and mud dispersal across continental shelves: Reappraising sediment transport processes operating in ancient mudstone successions. *Geology* 38(10), 947-950.

Macquaker J. H. S. and Bohacs K. M. (2007) On the accumulation of mud. *Science* 318, 1734-1735.

McCauley A. D. (2013) Sequence Stratigraphy, Depositional History, and Hydrocarbon Potential of the Mancos Shale, Uinta Basin, Utah. The University of Utah MS. Thesis.

Mulder T. and Alexander J. (2001) The physical character of subaqueous sedimentary density flows and their deposits. *Sedimentology* 48, 269-299.

Mulder T., Syvitski J. P. M., Migeon S., Faugeres J. C. and Savoye B. (2003) Marine hyperpycnal flows: initiation, behavior and related deposits. A review. *Mar. Petrol. Geol.* 20, 861-882.

Myrow P. M. and Southard J. B. (1996) Tempestite deposition. *J. Sediment. Res.* 66(5), 875-887.

Otto-Bliesner B. L., Brady E. C. and Shields C. (2002) Late Cretaceous ocean: Coupled simulations with the National Center for Atmospheric Research Climate System Model. *J. Geophys. Res.* 107(D2), ACL 11-1-ACL 11-14.

Pasley M. A., Riley G. W. and Nummedal D. (1993) Sequence Stratigraphic Significance of Organic Matter Variations: Example from the Upper Cretaceous Mancos Shale of the San Juan Basin, New Mexico in Katz B. J. and Pratt R. M., Source Rocks in a Sequence Stratigraphic Framework. AAPG Studies in Geology, 221-241.

Ridgley J. L., Condon S. M. and Hatch J. R. (2013) Geology and oil and gas assessment of the Mancos-Menefee Composite Total Petroleum System: Chapter 4 in Total petroleum systems and geologic assessment of undiscovered oil and gas resources in the San Juan Basin Province, exclusive of Paleozoic rocks, New Mexico and Colorado: U.S. Geological Survey, Digital data series 69-F, Chapter 4, 97 p.

Savrda C. E., BOTTJER D. J. and Gorsline D. S. (1984) Development of a Comprehensive Oxygen-Deficient Marine Biofacies Model: Evidence from Santa Monica, San Pedro, and Santa Barbara Basins, California Continental Borderland. *Am. Assoc. Pet. Geol. Bull.* 68(9), 1179-1192.

Savrda C. E. and Bottjer D. J. (1991) Oxygen-related biofacies in marine strata: an overview and update. *Geol. Soc. London Spec. Publ.* 58, 201-219.

Schieber J. (2016) Mud re-distribution in epicontinental basins — Exploring likely processes. *Mar. Pet. Geol.* 71, 119-133.

Shanmugam G. (1997) The Bouma Sequence and the turbidite mind set. *Earth-Sci. Rev.* 42, 201-229.

Suter J.R. (2006). Facies models revisited. *Special Publication – Society for Sedimentary Geology* 84, 1-527.

Taylor A. M. and Goldring R. (1993) Description and analysis of bioturbation and ichnofabric. *J. Geol. Soc. London.* 150(1), 141-148.

Wilson R. D. and Schieber J. (2014) Muddy Prodeltaic Hyperpycnites In the Lower Genesee Group of Central New York, USA: Implications For Mud Transport In Epicontinental Seas. *J. Sediment. Res.* 84(10), 866-874.